CHAPTER 114

EXCITATION OF WAVES INSIDE A BOTTOMLESS HARBOR

by

Noboru Sakuma[1], Johannes Bühler[2] and R. L. Wiegel[3]

1. INTRODUCTION

In planning enclosed areas in the ocean, such as offshore harbors for fishing or recreational boats, one has to consider very carefully the problem of forced seiches due to surface water waves. A number of papers have been written on this problem, but to the authors' knowledge, only one of them has treated the case of an artificial bottomless circular harbor in the open ocean, for which the walls extend only part way to the sea floor. A bottom to such a harbor, which would be expensive, can only be omitted if the effect of its absence on the sea surface inside the harbor is not overly detrimental.

C.J.R. Garrett (1970) made a theoretical study of the excitation of waves inside such a harbor for the 'no-entrance' case. The object of this paper is to evaluate experimentally the behavior of the sea surface inside such a harbor, to compare the results with the theoretical values obtained by Garrett, and to extend the observations to the case for which there is an entrance to the harbor.

2. THEORY

A theory of the excitation of waves inside a partially immersed bottomless vertical circular cylinder was developed by C.J.R. Garrett. In this theory, the free surface displacement may be described by real partof $\zeta e^{-i\sigma t}$, where the incident wave is given by

$$\zeta = \zeta_o e^{ikx} \qquad (2.1)$$

$$= \zeta_o \sum_{m=o}^{\infty} \epsilon_m i^m J_m (kr) \cos m\theta \qquad (2.2)$$

where $\epsilon_o = 1$, and $\epsilon_m = 2$ for $m \geq 1$; ζ_o is the amplitude of the incident wave. Disturbances within a circular cylinder can be expressed approximately by

1 Research Engineer, Public Works Research Institute, Ministry of Construction, Japan (formerly graduate student, Dept. of Civil Engrg., Univ. of California, Berkeley, California

2 Graduate student, Dept. of Civil Engrg., Univ. of California, Berkeley, California

3 Professor, Dept. of Civil Engrg., Univ. of California, Berkeley, California

$$\zeta(r,\theta) = \zeta_o \sum_{m=o}^{\infty} \epsilon_m\, i^m\, \chi_m(r) \cos m\theta \tag{2.3}$$

The corresponding displacement potential (the product of $\frac{1}{-i\sigma}$ and the velocity potential) is

$$\zeta(r,\theta,z) = \zeta_o \sum_{m=o}^{\infty} \epsilon_m\, i^m\, \psi_m(r,z) \cos m\theta \tag{2.4}$$

where

$$\chi_m(r) = \frac{\partial\psi_m}{\partial z}\Big|_{z=d} \tag{2.5}$$

In order to satisfy the kinematic free surface condition, φ must also satisfy

$$\nabla^2 \varphi = 0 \tag{2.6}$$

$$\sigma^2 \varphi - g\frac{\partial \varphi}{\partial z} = 0 \quad \text{on } z = d \tag{2.7}$$

$$\frac{\partial \varphi}{\partial z} = 0 \qquad \text{on } z = 0 \tag{2.8}$$

$$\frac{\partial \varphi}{\partial r} = 0 \quad \text{on } r = a \text{ for } h \leq z \leq d \tag{2.9}$$

Garrett found that the appropriate expansion of ψ_m could be expressed as follows. In $r \geq a$

$$\psi_m(r,z) = J_m(kr) - \frac{J_m'(ka)}{H_m'(ka)} H_m(kr) \frac{Z_k(z)}{Z_k'(z)} + \sum_{\alpha} F_{m\alpha} \frac{K_m(\alpha r)}{\alpha K_m'(\alpha a)} Z_\alpha(z) \tag{2.10}$$

where

J_m, Y_m; ordinary Bessel functions

I_m, K_m; modified Bessel functions

$H_m = J_m + iY_m$; the Hankel function of the first kind

$$Z_k(z) = N_k^{-\frac{1}{2}} \cosh kz \tag{2.11}$$

$$Z_\alpha(z) = N_\alpha^{-\frac{1}{2}} \cos \alpha z \tag{2.12}$$

$$N_k = \tfrac{1}{2}\,[1 + (\sinh 2kd/2kd)] \tag{2.13}$$

$$N_\alpha = \tfrac{1}{2}\,[1 + (\sin 2\alpha d/2\alpha d\,)] \tag{2.14}$$

$$F_{m\alpha} = \frac{1}{d}\int_0^h f_m(z)\; Z_\alpha(z)\; dz \tag{2.15}$$

In $r \leq a$

$$\psi_m(r,z) = \sum_\alpha F_{m\alpha}\,\frac{I_m(\alpha r)}{I_m'(\alpha a)}\,Z_\alpha(z) \tag{2.16}$$

Using Eqs. (2.5) and (2.16), the free surface elevation of Eq. (2.3) is, for $r \leq a$

$$\chi_m(r) = A_m J_m(kr) + \sum_\alpha{}' F_{m\alpha}\,\frac{I_m(\alpha r)}{\alpha I_m'(\alpha a)}\,Z_\alpha'(d) \tag{2.17}$$

where

$$A_m = F_{mk}\,\frac{Z_k'(d)}{kJ_m'(ka)} \tag{2.18}$$

The solution for $r \geq a$ may be written

$$\chi_m(r) = J_m(kr) + B_m H_m(kr) + \sum_\alpha{}' F_{m\alpha}\,\frac{K_m(\alpha r)}{\alpha K_m(\alpha a)}\,Z_\alpha'(d) \tag{2.19}$$

where

$$B_m = (A_m - 1)\,\frac{J_m'(ka)}{H_m'(ka)} \tag{2.20}$$

The first term on the right hand side of Eq. (2.17) is the most important contribution to the wave motion inside the cylinder; the other terms describe waves which are generally confined near $r = a$.

Garrett made numerical calculations of A_m for several conditions. These have been reproduced in Figs. 1 and 2, in order that they can be compared with experimental results.

3. EXPERIMENTAL ARRANGEMENTS AND PROCEDURE

The experimental study reported herein was made in the hydraulic model basin (150 ft. by 63 ft. by 2½ ft.) at the Richmond Field Station of the University of California.

3.1 Conditions Tested

The conditions that were tested in the experiment are as follows (for definition of the symbols, see Fig. 3):

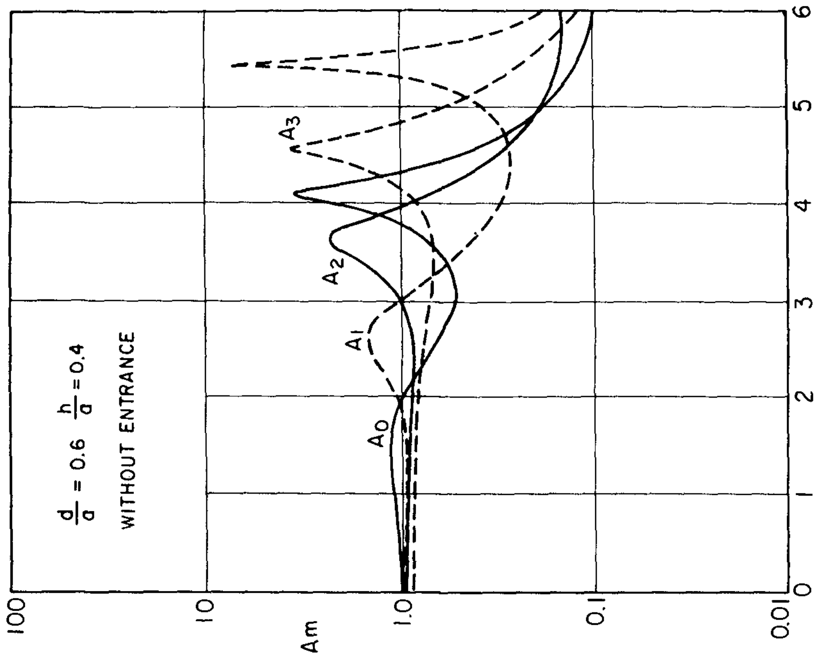

FIG. 2 THEORETICAL VALUES OF Am VS. ka
(from Garrett)

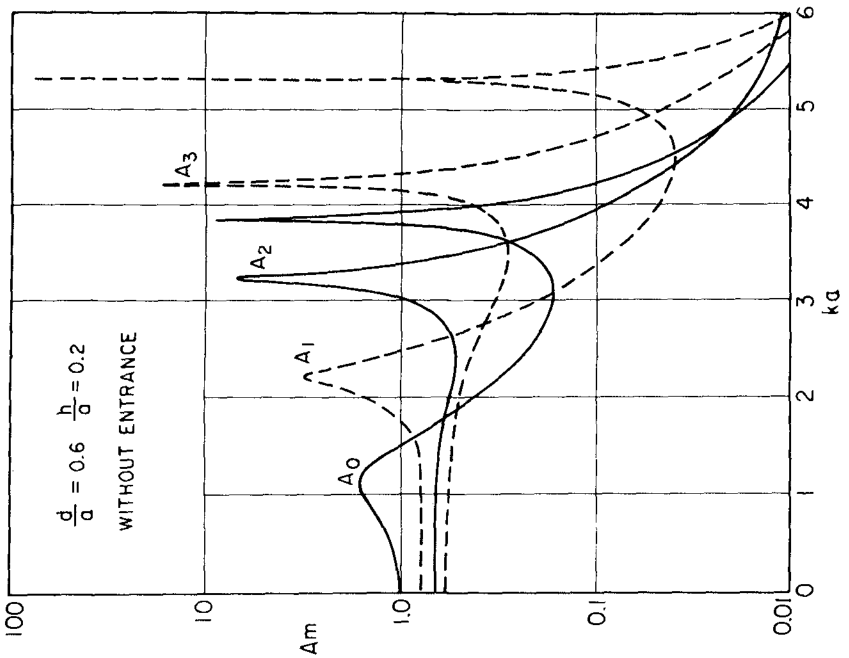

FIG. 1 THEORETICAL VALUES OF Am VS. ka
(from Garrett)

CASE NO.	$\frac{d}{a}$	$\frac{h}{a}$	NOTES
1	0.6	0.2	Without entrance.
2	0.6	0.4	
3	0.6	0.2	With an entrance in the rear.
4	0.6	0.4	
5	0.6	0.2	With an entrance on the side.
6	0.6	0.4	
7	0.6	0.2	With an entrance at the front.
8	0.6	0.4	

with d = 0.9 ft.; a = 1.5 ft.; h = 0.3 ft., and $ka = 2\pi a/L = 0.5 \sim 8.0$.

Two different experimental arrangements were used. The first series of experiments were conducted in a section of the model basin for cases 1 and 2. This arrangement is shown in Fig. 4 (small basin). The experiments were then repeated with an arrangement as shown in Fig. 5 (large basin) and the results compared. Because of the reduced reflection effects, the remaining cases were then studied in the large basin.

3.2 Experimental Arrangements and Procedures

Wave heights and wave periods inside and outside the cylinder were measured by means of parallel wire resistance type wave gages and a multichannel rectilinear writing oscillograph (Wiegel, 1953).

Four wave gages were used to measure the waves; one was used to measure the incident waves, and three were used to measure the waves inside the cylinder. The wave gage that was used for measuring incident waves was installed as far away from the cylinder as possible in the model basin in order to minimize the effect of wave reflection from the cylinder (see Figs. 4 and 5). The other three wave gages were installed inside the cylinder to enable measurement of the maximum wave height for each mode of harbor water surface oscillation.

In measuring the forced surface oscillations inside the cylinder and in interpreting the results, it is useful to consider the modes of oscillation to be the same as the modes of free oscillation inside a vertical circular harbor which extends to the bottom. This case has been studied theoretically and experimentally by J. S. McNown (1951; 1952) and by Goda (1963). The water surface elevations inside a vertical circular cylinder are expressed as

$$\zeta = C_m J_m(kr) \cos m\theta \qquad (3.1)$$

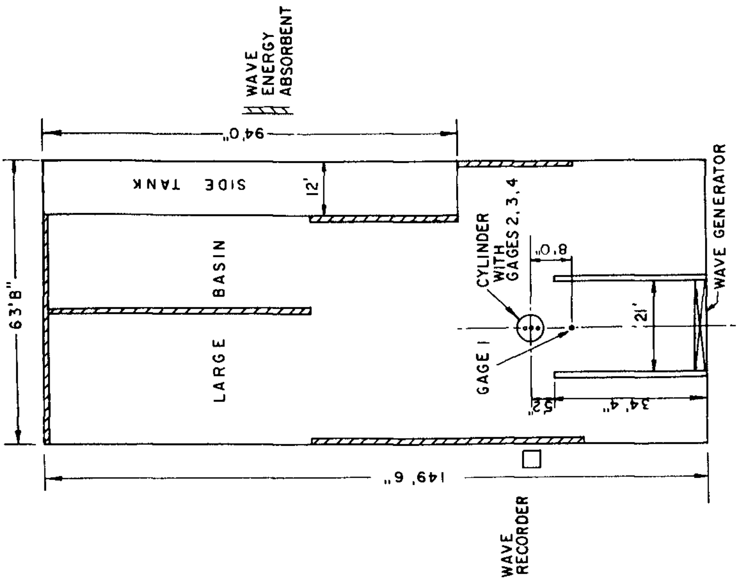

FIG. 5 EXPERIMENTAL ARRANGEMENT LARGE BASIN

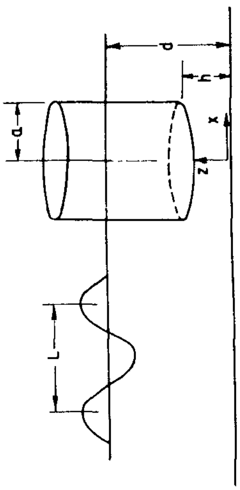

FIG. 3 DEFINITION SKETCH OF BOTTOMLESS VERTICAL CIRCULAR CYLINDER PARTIALLY IMMERSED

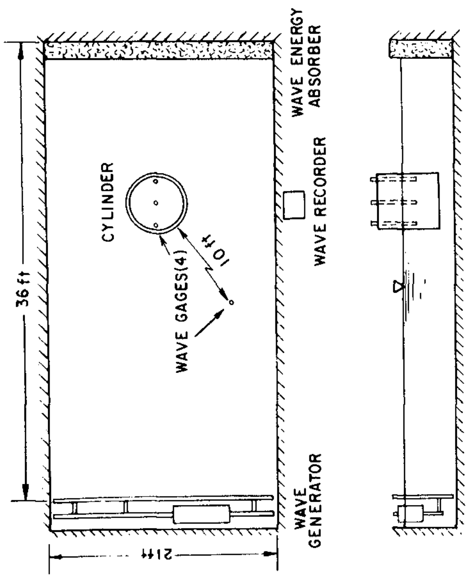

FIG. 4 EXPERIMENTAL ARRANGEMENT SMALL BASIN

where C_m is a coefficient related to the wave amplitude, k is the wave number $(2\pi/L)$, L is the incident wave length, r is the radial coordinate, θ is the angular coordinate, m is an integer and J_m is the Bessel's function of order m. Some of the possible modes expressed by the above expression are shown in Fig. 6.

In the experiment, however, it appeared that the mode or modes occurring within the cylinder were mostly of the lowest order of m; in other words, 0_1, 1_0, 2_0, 3_0 (Fig. 10) were observed, even though theoretically the number of modes possible for a given value of ka is infinite.

The places where the maximum wave elevation were observed in the cylinder were either at the center of the cylinder or near the wall of the cylinder. The orientation of the nodal lines of mode 1_0, for instance, would be normal to the direction of advance of incident waves. Therefore, for almost all of the experimental runs the three gages inside the cylinder were installed as shown in Fig. 7.

The cylinder which was used as a model of a circular harbor was made of steel and had three legs to hold it at the desired elevation above the bottom. After a number of measurements were made, an entrance to the harbor was made by cutting out a section of the cylinder, as shown in Fig. 8. For additional measurements without an entrance, the section was put back in place and the gaps closed with a plastic sealant.

An example of an incident wave record is shown in Fig. 9. It was difficult to define a "height of the incident wave," especially at higher wave numbers ka. When the generator was started, the waves gradually increased in height. The effects of reflection became evident before a uniform height was reached. The incident wave height was defined as the equilibrium wave height after a long time. This includes reflections from the walls of the basin and the cylinder itself. The final tests were made in the large basin in order to minimize the effect of these reflections. Reproductions of the records of representative samples of nearly all conditions have been reproduced in a laboratory report (Sakuma, Bühler and Wiegel, 1971).

From this incident wave height ζ_o, the corresponding values of A_m' can be calculated as follows. From Eq. 2.17, except near the wall, $X_m(r)$ can be approximated by

$$X_m(r) = A_m J_m(kr) \tag{4.1}$$

as the first term on the right hand side of Eq. 2.17, $A_m J_m(kr)$, is a much more important contribution to the wave motion inside the cylinder than is the second term. Substituting Eq. 4.1 into Eq. 2.3 results in

$$\zeta(r,\theta) \doteqdot \zeta_o \sum_{m=o}^{\infty} \epsilon_m i^m A_m J_m(kr) \cdot \cos m\theta \tag{4.2}$$

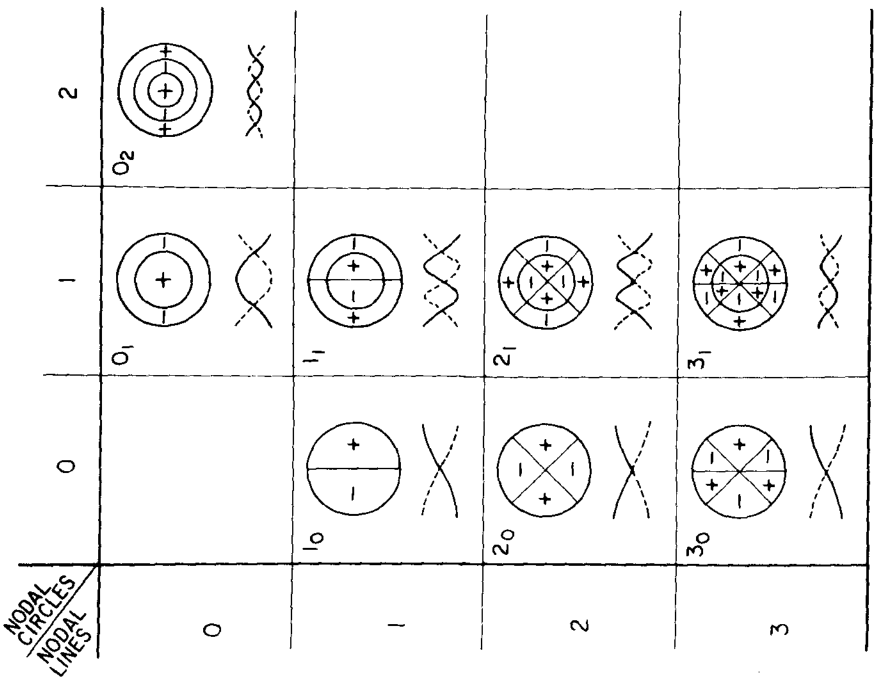

FIG. 6 SOME MODES OF FREE OSCILLATIONS IN A VERTICAL CYLINDER

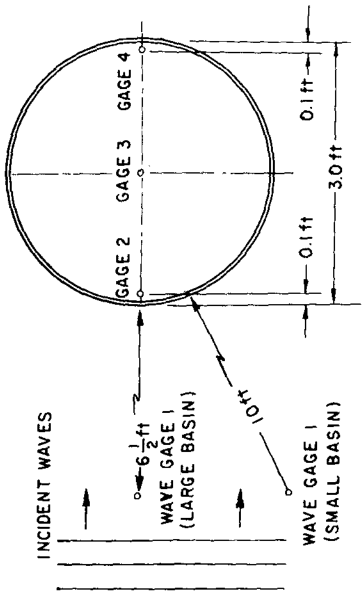

FIG. 7 WAVE GAGE LOCATIONS

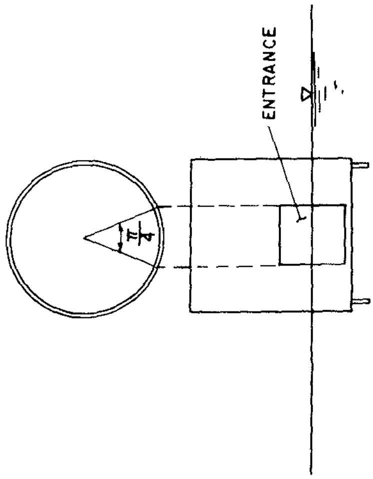

FIG. 8 CYLINDER WITH ENTRANCE

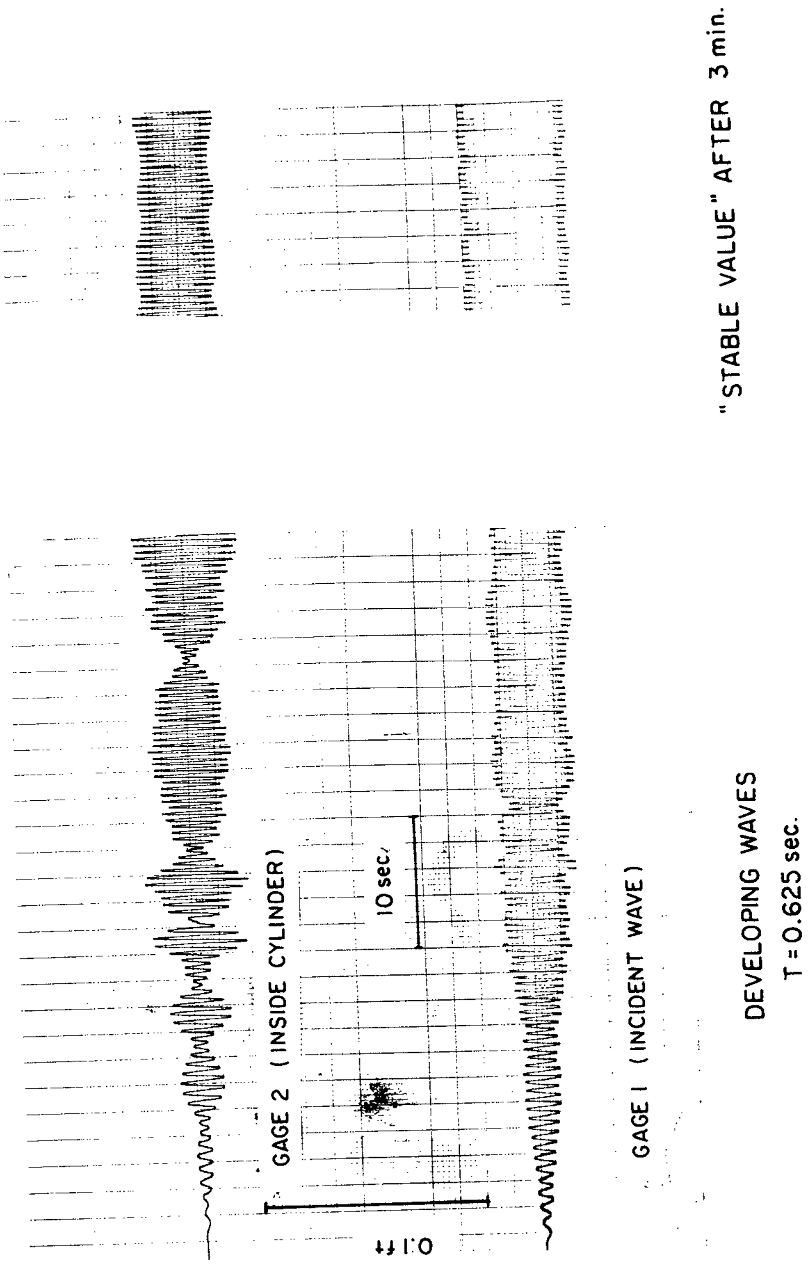

FIG. 9 EXAMPLE OF WAVE RECORD

so

$$Am = \frac{\zeta(r,\theta)}{\zeta_o \sum_{m=o}^{\infty} \epsilon_m \, i^m J_m(kr) \cdot \cos m\theta} \tag{4.3}$$

where $\epsilon_o = 1$, and $\epsilon_m = 2$ for $m \geq 1$. Defining A_m' as

$$A_m' = \frac{\zeta_{max}(r,\theta)}{\zeta_o \sum_{m=o}^{\infty} \epsilon_m \, i^m \, [J_m(kr)]_{max}} \tag{4.4}$$

with $[\cos m\theta]_{max} = 1$, and $\zeta_{max}(r,\theta)$ is the maximum wave height in the cylinder.

When $m = o$, Eq. 4.4 will be

$$A_o' = \frac{\zeta_{max}(r,\theta)}{\zeta_o [J_o(kr)]_{max}} \tag{4.5}$$

$$= \frac{\zeta_{max}(r,\theta)}{\zeta_o} \tag{4.6}$$

since $[J_o(kr)$ max $= 1$.

When $m = 1$:

$$A_1' = \frac{\zeta_{max}(r,\theta)}{2 \; \zeta_o [J_1(kr)\;]_{max}} \tag{4.7}$$

$$= \frac{\zeta_{max}(r,\theta)}{2(0.58)\; \zeta_o} \tag{4.8}$$

$$= 0.86 \; \frac{\zeta_{max}(r,\theta)}{\zeta_o} \tag{4.9}$$

when $m = 2$:

$$A_2' = \frac{\zeta_{max}(r,\theta)}{2 \; \zeta_o \; [J_2(kr)\;]_{max}} \tag{4.10}$$

$$= \frac{\zeta_{max}(r,\theta)}{2 \; \zeta_o [J_3(kr)_{max}} \tag{4.11}$$

$$= 1.04 \; \frac{\zeta_{max}(r,\theta)}{\zeta_o} \tag{4.12}$$

when m = 3

$$A_3' = \frac{\zeta_{max}(r\theta)}{2\ \zeta_o [J_3(kr)]_{max}} \tag{4.13}$$

$$= \frac{\zeta_{max}'(r,\theta)}{2(0.44)\ \zeta_o} \tag{4.14}$$

$$= 1.14\ \frac{\zeta_{max}(r,\theta)}{\zeta_o} \tag{4.15}$$

and so on.

As stated previously, the modes of oscillation which were observed in the cylinder were mostly of the J_0, J_1, J_2, J_3 types, or a combination of two or more of these modes. The fact that higher modes of oscillation were not observed, combined with the likely accuracy of the experimental measurements, A_m' can be approximated by:

$$A_m' \approx \frac{\zeta_{max}(r,\theta)}{\zeta_o} \tag{4.16}$$

for most practical purposes. This approximation was used to calculate A_m' as shown in Figs. 12 - 18.

4. RESULTS AND DISCUSSION

4.1 Small Basin

The results obtained for the small basin are shown in Figs. 12 and 13.

Each observed mode of oscillation is assigned a symbol. The symbols are defined in Fig. 10. The modes were recognized by a combination of visual observation and a study of the recordings of the outputs of the three wave gages within the cylinder. Generally, it was very difficult to tell which mode or modes of oscillation were occurring in the cylinder; sometimes two or more were observed at the same time, especially for the case of the cylinder with an entrance. As stated before, the modes recognized in the cylinder were either one of the lowest order possible or a combination of two or more such modes. Modes of higher orders might have existed in the cylinder in the experiment but they were not clear enough to be recognized. The orientation of the observed nodal lines were as shown in Fig. 10.

One has to be careful about ζ_{max}. For mode 1_0, for example, one would expect that the wave height at the location where wave gage #2 was installed would be the same as the wave height at wave gage #4 for the "no entrance" case. However, it was found that the wave height at wave gage #4 was larger than the height at wave gage #2 except for ka > 4.5 with h/a = 0.2 (Fig. 11, Small Basin). It is important to note in this regard that McNown (1951; 1952) found such a non-symmetry for the case of waves with a period close to two resonant conditions having nearly equal periods.

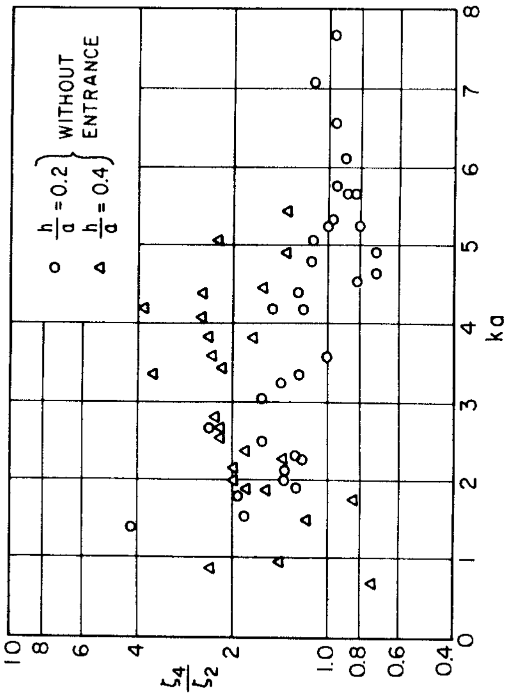

FIG. 11 RATIO OF WAVE HEIGHTS, WAVE GAGES 2 AND 4 SMALL BASIN

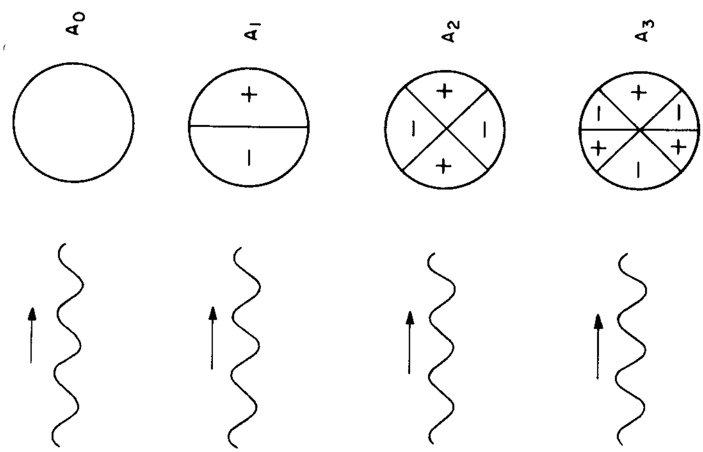

FIG. 10 OBSERVED ORIENTATIONS OF NODAL LINES

In calculating values of A_m' , the maximum value of ξ observed at any one of the 3 gages was used.

Consider the theoretical and experimental results for case 1 with $h/a = 0.2$ as shown in Figs. 1 and 12. The resonance patterns are alike; the values of ka for which peaks for different modes of oscillation appear in Fig. 12 are very similar to those in Fig. 1. The calculated response curves show very sharp peaks for the larger values of ka, while a substantial damping effect is apparent in the experiment data.

In regard to the results for case 2 with $h/a = 0.4$ (see Figs. 2 and 13), the damping effect is smaller than for the case of $h/a = 0.2$. In addition, the ratio of the wave height at wave gage #4 to the wave height at wave gage #2 is larger compared with the case of $h/a = 0.2$ (Fig. 11). The maximum value of A_m' is about the same for both cases. $A_m' = 2.5 \sim 2.8$.

4.2 Large Basin

The results for cases 1 and 2 are shown in Figures 12 and 13. The modes of oscillation agreed well with the ones observed in the small basin for corresponding wave numbers. The peak values of A_m' appear at the same values of ka as for the small basin.

The values of A_m' for ka > 3 are smaller for the large basin. This is mainly due to reflections from the back wall of the small basin.

As third and fourth case, a bottomless, vertical circular cylinder with an entrance in the rear was studied (see McNown, 1951 and 1952, for a theoretical and laboratory study of a circular cylindrical harbor extending to the bottom). The authors are not aware of any theoretical studies of this case. Figs. 14 and 15 show the experimental results, with no designation for different modes of oscillation as the modes observed in the cylinder were not clear. The surface oscillations within the cylinder appeared to be a combination of two or more modes, and, in addition, were affected by the disturbances due to the flow through the entrance.

It is interesting to note that a nodal line did not form at the entrance; instead, quite a large amplitude of oscillation was observed. Wave diffraction was observed at the entrance. The wave heights are generally smaller than for the harbor without entrance except at high wave numbers for $h/a = 0.2$ (Fig. 14). The peak value at ha $= 4$ in Fig. 14 is not well defined, amplitude of the incident wave was fluctuating.

Figures 16 and 17 show the behavior of the harbor with the entrance in different locations. For the entrance in the rear, the oscillations inside the harbor decrease rapidly with increasing wave number. For the entrance at the front, the oscillations are larger at high wave numbers. The high peaks near ka $= 4$ and ka $= 7$ are not well defined. The maximum and minimum values of 5 runs are connected by vertical bars to give an estimate of the width of the fluctuations. The recordings of both incident

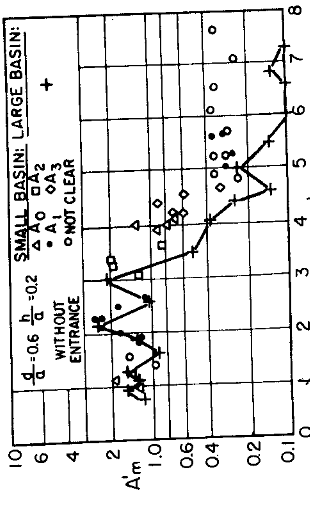

FIG 12 EXPERIMENTAL VALUES OF A'_m vs ka WITHOUT ENTRANCE, d/a = 0.6 h/a = 0.2

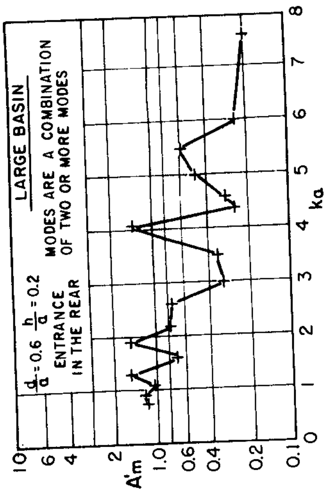

FIG 14 EXPERIMENTAL VALUES OF A'_m vs ka WITH ENTRANCE, d/a_o = 0.6 h/a = 0.2

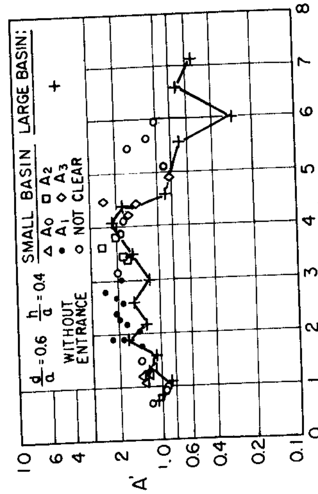

FIG 13 EXPERIMENTAL VALUES OF A'_m vs ka WITHOUT ENTRANCE, d/a = 0.6 h/a = 0.4

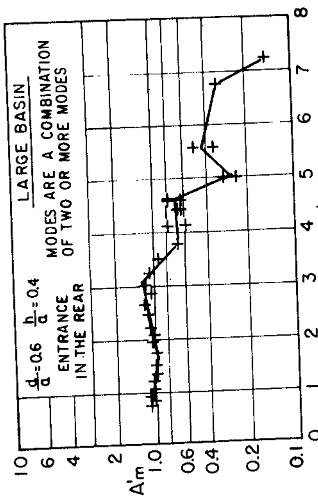

FIG 15 EXPERIMENTAL VALUES OF A'_m vs ka WITH ENTRANCE, d/a = 0.6 h/a = 0.4

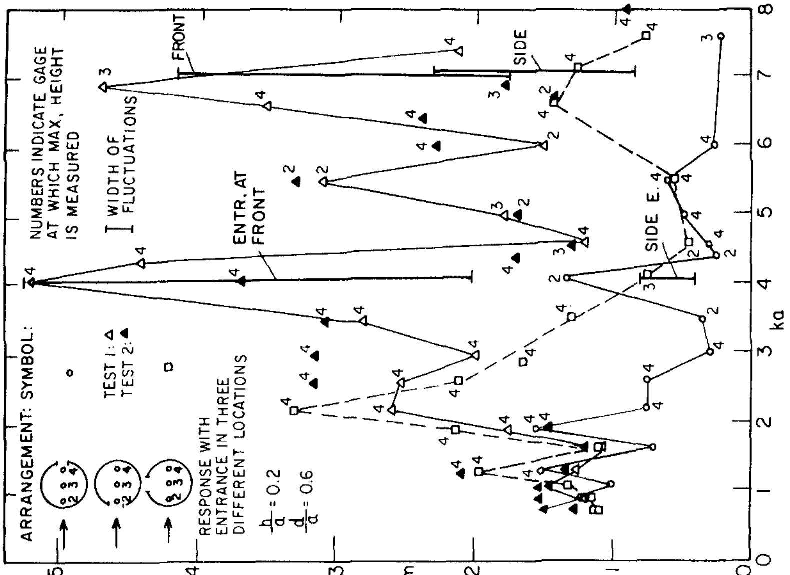

FIG.16 EXPERIMENTAL VALUES OF A'm vs ka

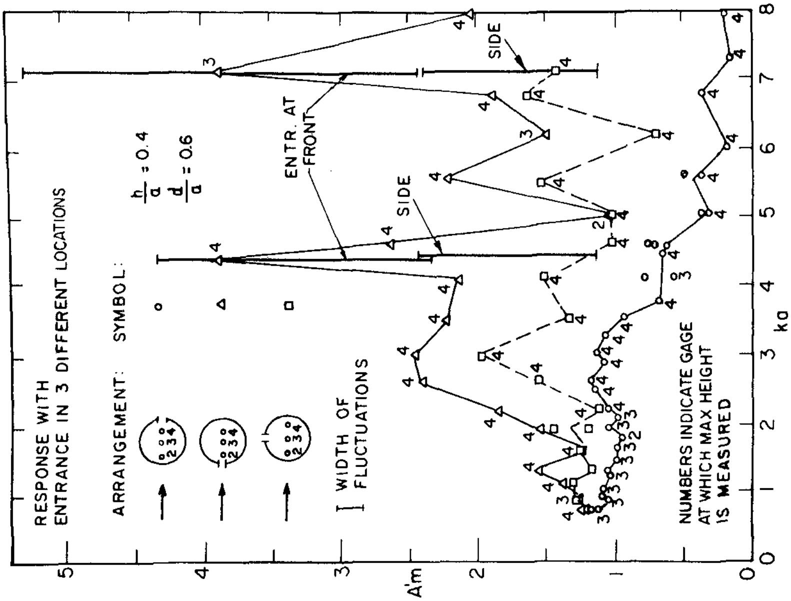

FIG.17 EXPERIMENTAL VALUES OF A'm vs ka

wave height and harbor oscillations showed large amplitude fluctuations at these values of ka. It was evident from observations made during the tests that reflections were the cause of this behavior.

Fig. 18 shows the maximum values of A_m for 3 different gage arrangements for the harbor with the entrance on the side. The largest oscillations of the water level occur in the center of the harbor for low wave numbers and at the remote end of the harbor for high ones. It is thus concluded that even for the case of an entrance on the side, the arrangement of the gages parallel to the direction of wave incident gives the maximum wave heights.

5. CONCLUSIONS

5.1 Harbor Without Entrance

1) Waves having the values of ka for which the resonance peaks of the J_0, J_1, J_2, and J_3 modes occurred, were generated in the laboratory, as well as waves of a series of other values of ka. Resonant peaks were observed in the laboratory study for the same values of ka at which the theoretical resonant peaks occur.

2) Damping of the wave amplitudes within the cylinder was found to be relatively large in the laboratory experiments for the larger values of ka.

3) The results of the experiments made with the cylinder without an entrance show the maximum values of A_m' to be from 2.0 to 2.5 (large basin). The maximum values occur at wave numbers ka smaller than 4.

5.2 Harbor With an Entrance

1) The modes of oscillation were usually complex and could not be classified according to Fig. 10.

2) The measurements showed that the oscillations were smaller for an entrance in the rear than for all entrance at the front, especially for wave numbers ka larger than 2.0.

3) With an entrance in the rear, the maximum values of A_m' were 1.1 for $h/a = 0.4$ and 1.6 for $h/a = 0.2$. The maximum values were observed at wave numbers ka smaller than 4.0.

4) With an entrance on the side, a maximum value of A_m' was observed at a wave number ka between 2.0 and 3.0. This maximum value of a'm was 2.0 for $h/a = 0.4$ and 3.2 for $h/a = 0.2$.

5) With an entrance at the front, large amplitude fluctuations were observed near ka = 4.0 and ka = 7.0. As an example, the values of a'm ranged from 2.4 to 5.3 at ka = 6.8 for $h/a = 0.4$. The fluctuations were due to the reflection of waves from the boundaries of the basin.

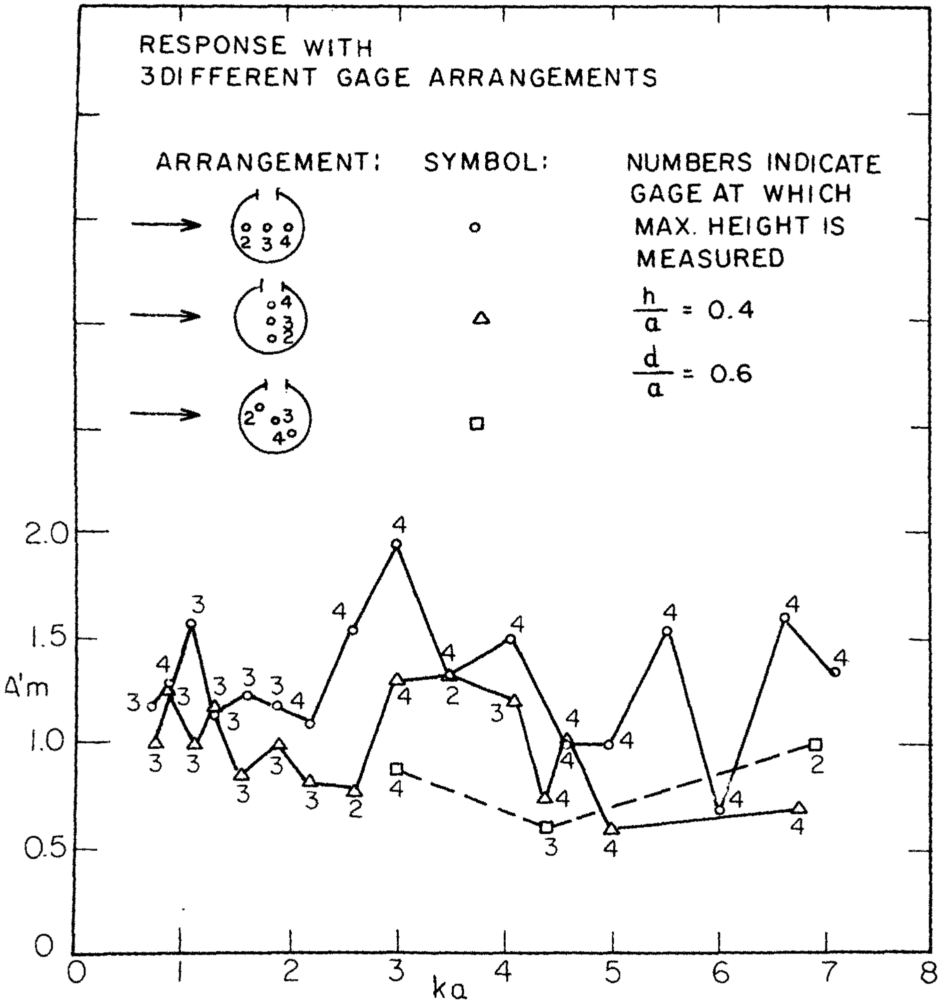

FIG.18 EXPERIMENTAL VALUES OF A'm vs ka

6. ACKNOWLEDGEMENTS

The senior author gratefully wishes to acknowledge the support of the Japan Public Works Research Institute, which made it possible for him to undertake graduate studies at the University of California.

The work reported herein was partially supported by the Coastal Engineering Research Center, Corps of Engineers, U.S. Army.

7. SYMBOLS

a = radius of circular cylinder

A_m = defined by Eq. (2.18)

B_m = defined by Eq. (2.20)

C_m = a coefficient related to the wave amplitude in Eq. (3.1)

d = water depth

g = acceleration of gravity

h = vertical distance from sea floor to bottom of cylinder

H_m = Hankel function of the first kind

I_m = modified Bessel function

J_m = ordinary Bessel function

k = wave number, $2\pi/L$

L = wave length

m = an integer, 0,1,2...

r = radial coordinate

T = wave period

x = horizontal coordinate in the direction of incident wave advance

z = vertical coordinate, $z = 0$ at undisturbed water surface

α = a real positive solution of $\alpha \tan \alpha d + \frac{\sigma^2}{g} = 0$

ϵ_m = a number; $\epsilon_o = 1$, and $\epsilon_m = 2$ for $m \geq 1$

ζ = water surface elevation

ζ_o = amplitude of incident waves

θ = angular coordinate

$\sum_{\alpha}$ = summation over α including α + -ik

$\sum_{\alpha}'$ = summation over only the real roots, i.e., α = -ik is excluded

σ = wave frequency, $2\pi/T$

$\varphi(r,\theta,z)$ = displacement potential

$\chi(r)$ = defined by Eqs. (2.17) and (2.19)

$\psi_m(r,z)$ = defined by Eq. (2.10)

8. REFERENCES

Garrett, C.J.R., "Bottomless Harbors," Journal of Fluid Mechanics, Vol. 43, Part 3, pp. 433-449, 1970.

Goda, Y., "On the Oscillations in a Rectangular Harbor and a Sector-Shaped One," The 10th Coastal Engineering Conference, Japan, 1963, in Japanese.

McNown, J.S., Sur l'entretien des Oscillations des Eaux Portuaires, sous l'Action de la Haute Mer., Thèse, Faculté des Sciences, Univ. Grenoble, France, August 1951.

McNown, J.S., "Waves and Seiche in Idealized Ports," Gravity Waves, U.S. Dept. of Commerce, National Bureau of Standards, Circular No. 521, 1952, pp. 1953-164.

Sakuma, Noboru, Johannes Bühler and R. L. Wiegel, Experimental Study of the Excitation of Waves Inside a Bottomless Harbor, Technical Report HEL 1-17, Hydraulic Engineering Laboratory, University of California, Berkeley, California, May 1971, 36 pp.

Wiegel, Robert L., Parallel Wire Resistance Wave Meter, Coastal Engineering Instruments, Council on Wave Research, The Engineering Foundation, 1953, pp. 39-43.

Wiegel, Robert L., Oceanographical Engineering, Prentice-Hall, Inc., Englewood Cliffs, N.J., 1964.